Kiebach, Ragnar; Luna-López, Jose Alberto; Dias, Guilherme Osvaldo; Aceves-Mijares, Mariano; Willibrordus Swart, Jacobus

Characterization of Silicon Rich Oxides with Tunable Optical Band Gap on Sapphire Substrates by Photoluminescence, UV/Vis and Raman Spectroscopy

Characterization of Silicon Rich Oxides with Tunable Optical Band Gap on Sapphire Substrates by Photoluminescence, UV/Vis and Raman Spectroscopy

Ragnar Kiebach,[1]* Jose Alberto Luna-López,[1] Guilherme Osvaldo Dias,[2] Mariano Aceves-Mijares,[1] Jacobus Willibrordus Swart[2]

[1] Instituto Nacional de Astrofísica, Óptica y Electrónica, Apdo. Postal 51, Puebla, Pue. 72000, México. rkie@inaoep.mx, Tel: +52 (222) 266-31-00, Fax:+52 (222) 247-05-17.

[2] Center for Semiconductor Components, State University of Campinas, mail box 6061, Campinas – São Paulo – Brazil

Abstract. A detailed analysis of the optical properties of silicon rich oxides (SRO) thin films and the factors that influence them is presented. SRO films with different Si content were synthesized via LPCVD (low pressure chemical vapor deposition) on sapphire substrates. Photoluminescence (PL), UV/Vis and Raman spectroscopy were used to characterize the samples. An intense emission in blue region was found. An interesting fact is that the optical band gap correlates linearly with the reactants ratio, which allows the tuning of the band gap. The influence of parameters such as substrate, Si content, annealing temperature and annealing time on the optical properties are discussed and the possible mechanisms of the photoluminescence are compared with our experimental data.
Key words. Silicon rich oxides, optical properties, photoluminiscence
Keywords: Silicon nano crystals, nanostructured materials, luminescence, Raman spectroscopy, silicon rich oxides.

Resumen. Se presenta un análisis detallado de las propiedades ópticas de películas delgadas de oxido de silicio rico en silicio (SRO) y los factores que tienen influencia en las propiedades físicas. Películas de SRO con diferente contenido de silicio fueron depositadas por LPCVD (Deposito químico en fase vapor a baja presión-low pressure chemical vapor deposition) sobre substratos de zafiro. Fotoluminiscencia (FL) espectroscopia UV/Vis y Raman se usaron para caracterizar las muestras. Se encontró una intensa emisión en la región azul. La característica más interesante es la banda prohibida óptica, que se correlaciona linealmente con la razón de los reactivos, lo cual permite el ajuste de la banda prohibida. Las influencias de los parámetros como el substrato, contenido de silicio, temperatura y tiempo de recocido en las propiedades ópticas se discuten y los posibles mecanismos de fotoluminiscencia son comparados con los datos experimentales.
Palabras clave. Óxidos de silicio, propiedades ópticas, fotoluminiscencia

Introduction

Si nano crystals (Si nc) embedded in a SiO_2 matrix are currently attracting much interest as a candidate for efficient light emitter devices [1-3]. Such devices are highly desirable for the integration of optical signal and electronic data processing circuits on the same chip. Moreover, its fabrication process is compatible with the present large-scale integration technologies [4,5]. The band gap of Si nc is enlarged with respect to the bulk material and an intense visible PL at room temperature is observed.

The PL spectra consist of intense emission peaks in the near infrared and visible regions. It was established that blue and green PL are caused by various emitting centers in the silicon oxide, while the nature of the intense PL in orange-red region is still discussed [6-8].

To obtain $Si-SiO_x$ (x<2) systems a large variety of techniques has been used: ion implantation of Si into SiO_2 [9,10], magnetron sputtering of Si and SiO_2 [11,12], thermal evaporation of SiO [13-14], laser ablation of Si targets [15-17], molecular epitaxy, PECVD (plasma enhanced chemical vapor deposition) and LPCVD.

The optical properties of the $Si-SiO_x$ differ due to the synthesis technique, indicating structural differences of the Si nano clusters and their environment [10]. Raman scattering measurements are frequently used to prove the presence of Si nc. With this fast and nondestructive method it is possible to determine whether silicon particles are amorphous or crystalline. Moreover, information about mean size (MS) and sizes distribution (SD) of nano crystallites can be obtained from the peak position and shape of the Raman band. For samples using Si wafers as substrates, Raman measurements must be undertaken with care. The difficulty is that the strong Raman peak from the crystalline Si (c-Si) substrate masks the signal of the Si nc. To avoid this problem we used sapphire substrates. Then, the obtained Raman data can clearly be related to the deposited thin film, not to the substrate.

In this paper we report about the PL of SRO films synthesized by LPCVD with different Si excess and different annealing times. Raman measurements were performed to investigate the structure, MS and SD of the Si clusters embedded in the SiO_2 matrix. Additionally the influence from the Si excess on the optical band gap was investigated. Interestingly an almost linear coherency between the reactants ratio and the optical band gap was found. With this knowledge it is possible to design SRO films with a specific optical band gap just by a ratio control of the reactants, a very interesting feature for an application as optical device.

Results

Photoluminescence

In Fig. 1a-c PL spectra for Ro = 10, Ro = 20 and Ro = 30 after different annealing times are shown. Three different bands can be found in the PL spectra, peaked at 1.7 eV (725 nm) (Red band (R-Band)), 2.4 eV (515 nm) (Green band (G-band) and 2.8 eV (440 nm) (Blue band (B-band)). The intensities increase with decreasing Si excess, a result that is in accordance with literature [10, 19-22]. The Intensity for Ro = 20 compared to Ro = 10 is two to three times higher, for Ro = 30 is ten times higher than for R = 10 (table 1).

In table 1 the PL intensities for all samples are listed. Additionally, the percentage of changes for the R-Band and the
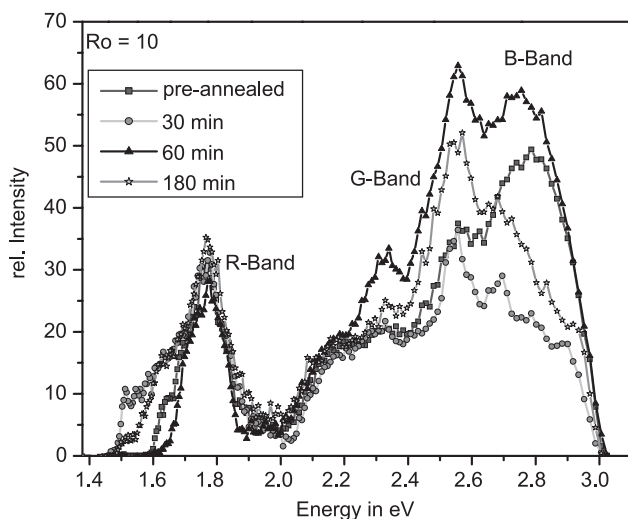

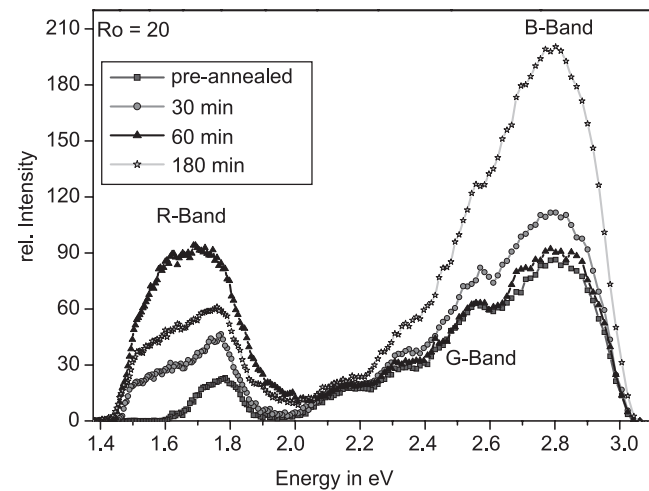**Fig. 1b.** Photoluminescence in the region from 1.4 eV to 3.1 eV for Ro = 20 after different annealing times

Fig. 1a. Photoluminescence in the region from 1.4 eV to 3.1 eV for Ro = 10 after different annealing times

Fig. 1c. Photoluminescence in the region from 1.4 eV to 3.1 eV for Ro = 30 after different annealing times
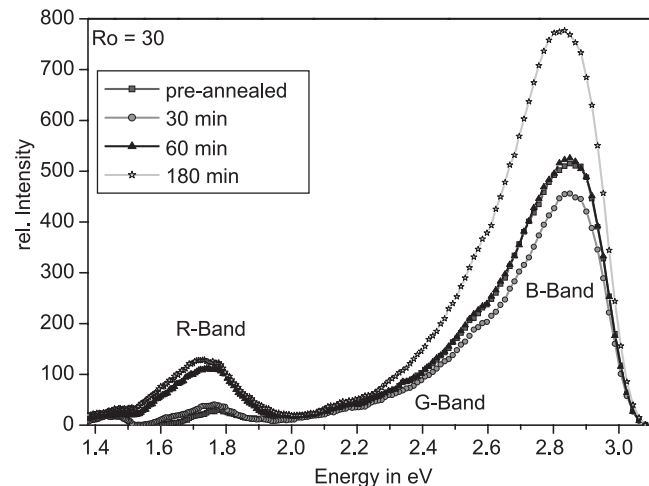
Table 1. Reaction conditions, *stoichiometry*, PL intensities and band gap of different samples

Sample name	Annealing time in min	Si excess* in %; formula	Intensity R-band in a.u., change in % in parentheses	Intensity B-Band in a.u., change in % in parentheses.	Band gap in eV
R10_0	0	11.7	31	49	1.63
R10_30	30	$SiO_{1.22}$	33 (+6.8)	23 (-53.7)	1.65
R10_60	60		28 (-8.3)	55 (+12.8)	1.65
R10_180	180		35 (+15.7)	29 (-41.7)	1.66
R20_0	0	8.7	22	84	2.37
R20_30	30	$SiO_{1.38}$	43 (+99.1)	112 (+33.5)	2.35
R20_60	60		91 (+321.3)	91 (+9.5)	2.42
R20_180	180		60 (+175.9)	200 (+139.5)	2.36
R30_0	0	5.5	13	514	2.64
R30_30	30	$SiO_{1.58}$	35 (+169.2)	451 (-12.4)	2.67
R30_60	60		107 (+723.1)	516 (+0.2)	2.65
R30_180	180		126 (+869.2)	772 (+49.9)	2.65

* Silicon excess (Si_{ex}) calculated from SiO_x with: $Si_{ex}(\%) = \left[\dfrac{100}{1+x}\right] - 33.3$

B-Band after annealing, compared to the pre-annealed samples, are presented. In general no consistent trend is observed.

For Ro = 10 no change in the R-band is observed, while the intensities of G-band and the B-band pass a maximum after 60 min of annealing, followed by decrease after further annealing, especially for the B-band. It has to be noticed that the intensity changes caused by annealing for Ro = 10 are small and almost negligible compared to Ro = 20 and Ro = 30. For Ro = 20 the R-band pass a maximum after 60 min of annealing. Annealing times up to 60 min only have small influence on the G-Band and the B-Band, but a significant increase is found after 180 min (table 1). The trend of the intensity changes caused by thermal treatment in the G-band and the B-band of the samples with Ro = 30 are comparable with the ones in Ro = 20, but the percental changes for Ro = 30 are more than three times higher. For the R-band an intensity increase with increasing annealing time is observed.

Raman spectroscopy

Raman scattering technique is commonly used for semi quantitative determination of the MS, SD and crystallinity of Si nc [22-24]. For each stoichiometry Raman spectra of the films heated at 1000 °C for 30 min, at 1100 °C for 30 min and at 1100 °C for 180 min were measured (table 2).

Amorphous silicon (a-Si) as well as c-Si can be identified by Raman spectroscopy. A broad band around ~ 480 cm^{-1} is typically associated to a-Si, while bulk silicon has a sharp peak around 521 cm^{-1}. For Si nc peak shifts to smaller wavenumber, as a function of decreasing size, has been widely reported due to quantum confinement effects.

For pre-annealed films with Ro = 20 and Ro = 30 no Raman peaks for Si nc were observed, but for Ro = 20 a broad band at 485 cm^{-1} indicates the presence of a-Si. Interestingly the sample with Ro = 10 shows an intense Raman peak for Si nc at 509.1 cm^{-1} (Fig. 2), indicating that for films with a high Si excess already during the 30 min of pre-annealing Si nc are formed. After 30 min of annealing at 1100 °C (Fig. 3) a small Raman peak around 521.1 cm^{-1} for Ro = 20 is observed (Fig. 3, inlet) while for Ro = 30 no peaks were found. Further heating treatment for another 150 min proceeds with this tendency, for Ro = 20 an increase of the intensity is observed whereas for Ro = 30 no characteristic peaks for Si phases are present. This shows that thermal annealing for samples with adequate Si excess favors the formation of Si nc, a result which accords with literature [23, 25].
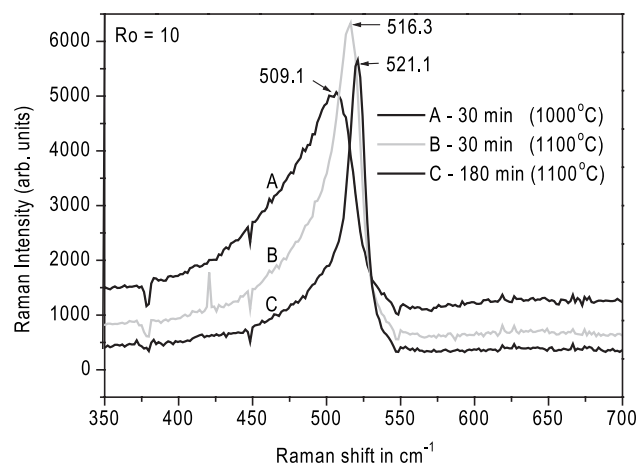

Fig. 2. Backscattering Raman spectra in the region from 350 cm-1 to 700 cm-1 for Ro = 10 after different annealing times
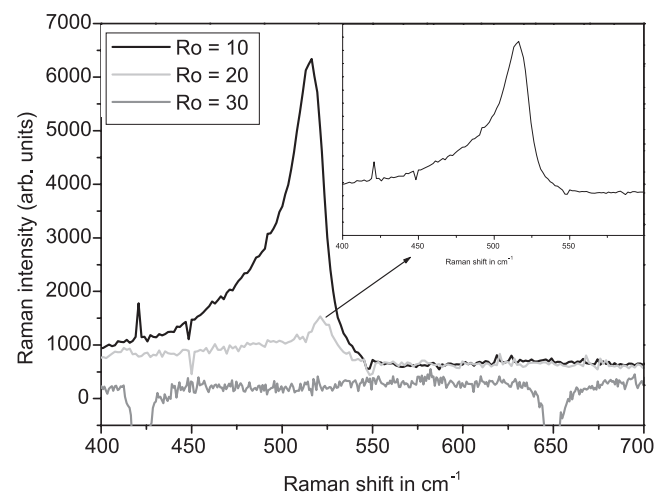

Fig. 3. Backscattering Raman spectra for Ro = 10, Ro = 20 and Ro = 30 after 30 min of annealing. The inlet shows a magnification of the Raman spectra for Ro = 20

A peak shift to higher wavenumber with increasing annealing time for the Raman peak of the Si nc in Ro = 10 indicates that Si nc are growing. After 30 min of annealing at 1100 °C a peak at 516.3 cm^{-1} was found, after 180 min of annealing the peak position at 521.1 cm^{-1} is comparable to the one of bulk Si (Fig.

Table 2. Overview about results from Raman spectra

Sample name	Annealing time (min.)	Temperature (°C)	Main peak (cm^{-1})	FWHM (cm^{-1})	Asymmetry (Γ_a/Γ_b)
Ro = 10	30	1000	509.1	41	3.00
Ro = 10	60	1100	516.3	16.7	1.55
Ro = 10	180	1100	521.1	10.06	1.4
Ro = 20	30	1000	485	168	2.04
Ro = 20	60	1100	521.1	31	1.93
Ro = 20	180	1100	519.5	12.4	1.14

2). For bulk silicon the Raman peak at ~ 521cm^{-1} corresponds to the frequency of the optical-phonon at the center of Brillouin zone, due to transition for momentum conservation. For Si nc the momentum is not well defined and transitions occur always at lower frequencies causing red shifts and widening in the Raman peak. The amount of these red shifts and widening depends of the MS, shape, and SD of Si nc (SD can be understood as metric dispersion around the MS of Si nc). Table 2 shows the position of the main Raman peak, Full Width Half Maximum (FWHM), and asymmetry (both last a measure of the width of the Raman peak). The asymmetry is defined as the ratio of half width toward lower frequencies (Γ_a) to that at higher frequencies (Γ_b). Asymmetry assigned as $\Gamma_a/\Gamma_b=1$ is associated with bulk crystalline materials (e.g., bulk silicon, which has a symmetrical Raman peak at ~ 521 cm^{-1}). One can see that after annealing the values of asymmetry and FWHM (for samples Ro = 10 and Ro = 20) decrease considerably, indicating that the SD of the Si nc decreases. Furthermore, the blue shifts observed for Ro = 10 indicates that the MS of the Si nc is increasing with the annealing time. If we suppose spherical Si nc, the peak located at 509.1 cm^{-1} corresponds to Si nc with a MS of ~ 3 nm (size dispersion about 30%). For a peak position at 516.3 cm^{-1} a MS around 5 nm can be assumed. Above this value the effects of red shifts and widening of the Raman peak are very weak [26]. For Ro = 20 the values for the peak position are similar to bulk Si; the asymmetry and FWHM decrease with the annealing time, suggesting decreasing in the size dispersion, but with the same MS.

For all samples containing c-Si an additional large band centered ~ 480 cm^{-1} as a result of the presence of amorphous silicon is found. To evaluate the development of the ratio between amorphous phase and Si nc phase the Raman spectra were fitted in a region between 400 cm^{-1} and 700 cm^{-1} (Fig. 4). To reproduce the crystalline peak an asymmetric Gaussian function was used taking the softening and broadening of the one phonon Raman peak under consideration [27]. The a-Si band was fitted by a Gaussian function and an additional polynomial function for the background was used. For the pre-annealed Ro = 10 film a relatively small a-Si/Si ratio of 0.445 is obtained, the values increase to 1.135 for 30 min and to 1.348 min for 180 min annealing at 1100 °C. For Ro = 20 after 30 min of annealing at 1100 °C a ratio of 3.524 is found, which decreases to 2.061 after 150 min of further annealing. In general one can say, that the a-Si/Si ratio for Ro = 20 is higher, but no unique tendency within the same stoichiometry is found.

Then, for samples having a sufficient amount of Si excess, it can be assumed that the excess Si is distributed in small clusters after the deposition. During the annealing in a first step bigger agglomerates of a-Si are formed. In a second step this agglomerates develop to crystalline structures like Si nc. But even after 180 min of annealing still a large amount of a-Si is found, indicating equilibrium between a-Si and c-Si.

UV/Vis spectroscopy

In Fig. 5 the UV/Vis transmittance spectra for all different Ro annealed at 1000 °C are shown. For all samples a sharp
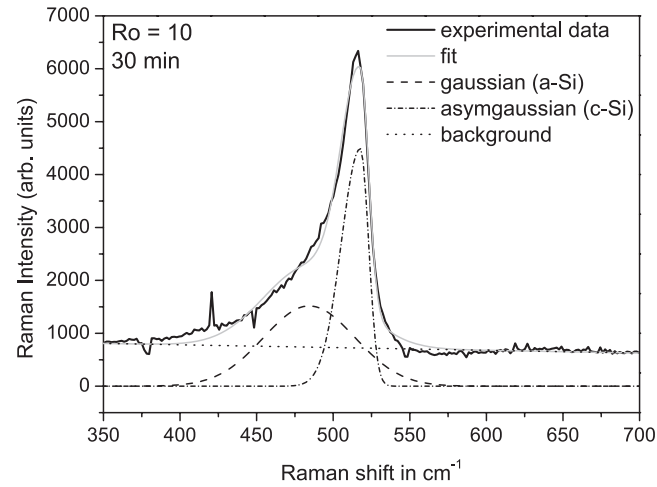

Fig. 4. Backscattering Raman spectra in the region from 350 cm-1 to 700 cm-1 of Ro = 10 after 180 min annealing with fit for crystalline and amorphous contributions

absorption edge is found. The position of the absorption edge differs significantly with the amount of the Si excess. A clear tendency is observable; an increase of the Si excess shifts the absorption edge towards shorter wavelength. Interestingly the influence of annealing has no noticeable influence on the absorption properties of these materials. In the UV/Vis spectra of the annealed samples (not shown) no significant changes are found.

The optical band gap Eg can be estimated from the following equation known as the Tauc plot [28]:
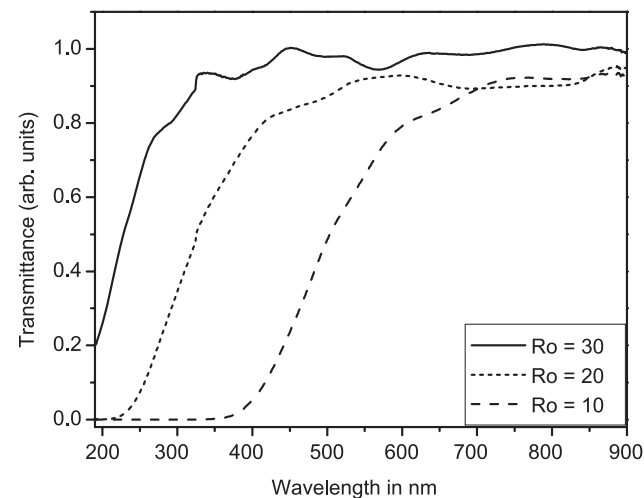
$$\alpha h\nu = A(h\nu - E_g)^n,$$

Fig. 5. UV/Vis transmittance spectra for Ro = 10, Ro = 20, Ro = 30 after densified at 1000 °C

where Eg is the band gap corresponding to a particular transition in the film, *A* is a constant, ν is the transmission frequency and the exponent *n* characterizes the nature of band transition. Values of *n* = 1/2 and 3/2 correspond to direct allowed and direct forbidden transitions, *n* = 2 and 3 are related to indirect allowed and indirect forbidden transitions [28]. From a plot $(\alpha h\nu)^{1/n}$ vs *hν* the band gap can be extrapolated from a straight line to *hν* = 0. For all different ratios and temperatures the best straight line is observed for n = 3 (Fig. 6), indicating an indirect forbidden transition mechanism.

The band gaps of all samples are above the one of c-Si (1.17 eV). A shift towards higher energy is observed for decreasing Si excess, for Ro = 10 a value of 1.63 eV, for Ro = 20 of 2.37 eV and for Ro = 30 of 2.64 eV is found. Interestingly the correlation between the band gap and the reactants ratio can be described as linear (Fig. 7). While the concentrations of the reactants have great influence on the value of the band gap, annealing again does not lead to significant changes. The values found differ not more than ± 0.05 eV for different thermal treatment (table 1).

Fig. 7. Correlation of the optical band gap with different Si concentrations/reactant ratios

Discussion

In the following part the influences of the substrate, the amount of the Si excess, the annealing temperature and annealing duration are discussed.

Influence of the substrate

The first factor, which has influence on the optical properties, is the substrate. In the PL spectra the unusual high intensity in the B-Band is remarkable. For experiments on Si substrates under the same deposition conditions the highest intensities are
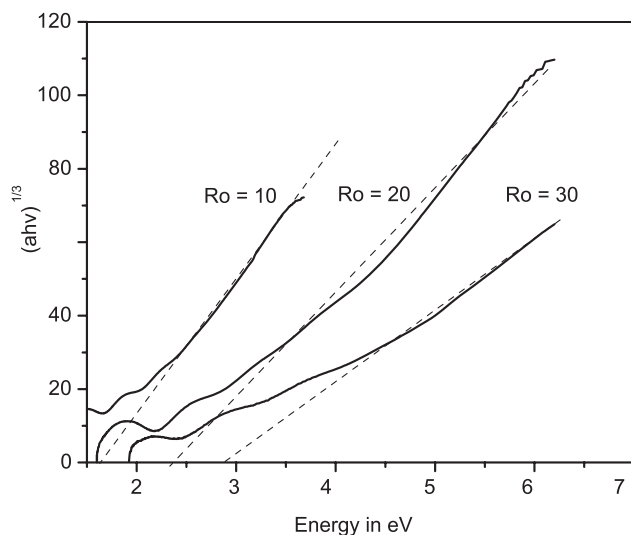

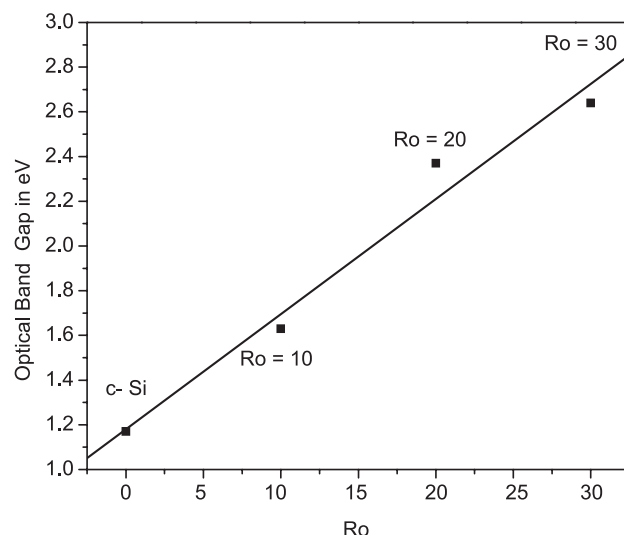**Fig. 6.** Tauc plots for n = 3 for Ro = 10, Ro = 20, Ro = 30. Dashed lines show the linear fit of the straight part

observed in R-Band. These results indicate that the substrate has influence on structural properties of the deposited SRO film. Rani et al. [17] compared the influence of different Si substrates (smooth and rough) on the PL. For rough substrates a blue shift and intensity increase were found. The explanations for this observation are different oxidation mechanisms leading to different termination of the Si nc. Si can be terminated by double bond to an oxygen atom (Si=O) or by a bond to hydroxyl group (Si-O-H), the energy gap and therewith the PL emission is different explaining the shift. In our case it can be assumed that the sapphire substrate is rougher than a Si wafer, which could explain a blue shift. But until now no experiment could proof a change in the amount of Si=O or of Si-O-H bonds undermining this theory. Compared with results for samples on Si substrates we published [10] the peak position of the B-band and the R-band are identical while their intensities differ strongly. Taking these results into consideration, it seems that the types of radiative channels are the same, but depending on the substrate specific defect structures are formed in the film preferential. Lin et al. [7] reported that neutral oxygen vacancies (NOV) $[O_3a\equiv Si\text{-}Sia\equiv O_3]$ are responsible for the emission in the B-band. Therefore sapphire substrates could lead to the formation of NOV explaining the high emission in the B-band.

Influence of the silicon content

The second factor is the Si content in the Si-SiO_x systems. The phase (crystalline or amorphous) and the structure (crystal size and distribution) of the Si nano crystallites and especially of their surrounding Si/SiO_2 interface have significant influence on the optical properties.

The observed PL intensity decrease, for the B-band as well as for the R-Band, with increasing silicon content is in accor-

dance to literature [10,19-22]. The low PL intensity found for Ro = 10 is typical for SRO materials with high silicon excess. Raman spectra for Ro = 10 (Fig. 3, 4) indicate a high content of c-Si. It can be assumed that the size of the crystalline areas is big enough to allow non-radiative recombination, comparable with recombination processes found in bulk Si, explaining the low PL intensity.

Also for Ro = 20, after annealing a Raman peak indicating the presence of a c-Si phase is found, but the intensity of this peak is low compared to Ro = 10. Interestingly also the PL is increasing with the annealing time, but it can be excluded that the observed Si nc are direct responsible for the strong PL. For Ro = 30 a much higher PL intensity is found (six to seven times higher) while no characteristic peak for c-Si is found.

These results assume that the Si/SiO_x species responsible for PL emission are not directly observable by Raman spectroscopy due to their small size [22] or their amorphous structure. It is possible that very small grains are invisible in Raman spectra due to their specific structural organization similarly to ultra thin amorphous layers [29]. It is also known that the ordering of small Si crystals depends on bonding of the surface atoms, and oxidized crystallites show stronger disorder [30]. In our case the appearance of peaks indicating c-Si in the Raman spectra should be interpreted as a phase separation between Si and SiO_2 induced by thermal annealing. These results support models considering defects in the interface between Si nc and the SiO_2 as emitting centers. The high PL intensity in Ro = 30 and Ro = 20 can be explained with small size and the disorder of the Si crystallites. In these samples the surrounding matrix should be more defect rich than the one found for large crystalline agglomerates of Si as proposed for Ro = 10.

Influence of annealing time and temperature

Other important factors are annealing temperature and annealing duration. Annealing seems to advantage the formation of c-Si (obtained by Raman) as well as the formation of (defect-) structures responsible for the PL emission (obtained by PL spectroscopy). While annealing has a strong influence on the PL, the influence on the band gap is almost negligible. This means that factors like particle size, morphology and phase separation have almost no impact on the band gap. Only the *stoichiometry* seems to have influence on the position of the absorption edge (table 1). Interestingly, the observed tendency that the band gap increases with increasing oxygen content is comparable with the tendency Chu et al. [31] calculated for HOMO-LUMO band gaps of small Si_xO_y clusters. Also in this calculation the band gap increases with higher oxygen content. The almost linear dependence from the band gap due to the reactants ratio makes it possible to synthesize materials with designed optical properties. But it has to be mentioned, that it is doubtful that this linear trend continues for higher Ro´s. The estimated value for SiO_2 following the linear relationship would be significant lower than that of ~ 8 eV for the band gap of bulk SiO_2.

The direct correlation between the PL and the band gap is difficult. Changing the amount of Si excess changes the position of the band gap while the peak positions (not the intensities) in the PL spectra are almost constant. For an understanding of these results the absorption process and the emission process must be regarded separately. An increase of the Si excess leads to a shift of the absorption edge, also light with larger wavelength is absorbed. Then again the wavelengths of the emission in the visible region do not shift, only their intensities vary. This means the type of radiative recombination channels do not change. Therefore a change in the non-radiative recombination processes can be expected with increasing Si content.

The large variety of factors which can be used to influence the optical properties makes these materials an interesting candidate for applications. A tuning of the band gap is possible by varying the reactants ratio. Furthermore, the PL emission can be, in a certain range, tuned by thermal annealing and the choice of the substrates in previous productions steps.

Conclusions

The influence of different factors on the optical properties of SRO has been discussed on experimental data. It has been found that the PL increases with annealing time and decreases with higher silicon excess. The use of sapphire as substrate leads to a strong PL in the blue region compared with samples on Si substrates. The formation and growth of Si nc and the formation of a-Si in samples with different Si:O ratios after different annealing times was investigated with Raman spectroscopy. The presence of a crystalline phase (Si nc) seems not to be necessary for the occurrence of photoluminescence. Interestingly it was found that the optical band gap strongly correlates with the Si:O ratio and is tunable over a large energy range via the reactant ration.

Experimental

Before deposition substrates were cleaned according to standard RCA procedure.

The SRO layers were deposited using LPCVD on sapphire (Al_2O_3) substrates. A hot wall reactor was used as reaction vessel and the pressure was controlled by mass flow controllers and a Baratron pressure sensor. A silane (SiH_4) and nitrous oxide (N_2O) mixture was used with different partial pressure ratios (Ro) according to:

$$Ro = \frac{p[N_2O]}{p[SiH_4]}.$$

Samples with three different Ro and therewith three different *stoichiometry* (Ro = 10 (~ $SiO_{1.22}$), Ro = 20 (~ $SiO_{1.38}$), Ro = 30 (~ $SiO_{1.58}$)) were synthesized. The silicon excess listed in table 1 is defined as the additional percental amount of Si in comparison with SiO_2 (SiO_2: 33.3 atomic % of silicon).

During deposition the substrate temperature was 700 °C. After deposition all samples were pre-annealed at 1000 °C for 30 min in nitrogen atmosphere to avoid aging effects [18]. After the first annealing step some samples were annealed at 1100 °C with different duration (table 1).

SRO films on n-type Si-Wafers were deposited under exactly the same reaction conditions for thickness measurements with an ellipsometer. The thickness of the SRO films is around 550 nm.

The thickness and refraction index of the SRO films were measured using a Gärtner L117 ellipsometer with incident laser wavelength of 632.8 nm.

Back-scattering Raman experiments were performed at room temperature, using a triple monochromator micro-Raman spectrometer (DILOR XY) and Ar-laser excitation line at 514.5 nm (2.41eV). A 100x microscope objective was used for focusing the laser beam on the sample and for collecting the scattered light. The laser spot has diameter of ~1μm on the sample and the power density was ~7x10^5 W/cm^2. The integration time was 100 s for each sample measurement.

PL at room temperature was carried out with a Perkin Elmer luminescence spectrometer model LS50B, which is controlled by computer. The samples were excited using a 250 nm (4.96 eV) radiation. PL measurements were scanned between 400 and 900 nm (3.1–1.37 eV) with a resolution of 2.5 nm.

Optical transmittance measurements were made in the range of the UV to near infrared at room temperature, using a spectrophotometer Perkin-Elmer LMBD 3B UV/VIS.

Acknowledgment

Supporting Information Available

Tauc plot for different values of n; first derivation of the; Tauc plots with details of the fitting procedure; PL spectra of SRO films on sapphire and Si Wafer in comparison.

References

1. Nayfeh, M.; Rao, S.; Barry, N.; Therrien, J.; Belomoin, G.; Smith, A.; Chaieb, S. *Appl. Phys. Lett.* **2002**, *79*, 1249-1251.

2. Pavesi, L.; Dal Negro, L.; Mazzoleni, C.; Franzo, G.; Priolo, F. *Nature* **2000**, *480*, 440-444.

3. Luterova, K.; Pelant, I.; Mikulskas, I.; Tomaisiunas, R.; Mueller, D.; Grob, J.-J.; Rehspringer, J.-L.; Honerlage, B. *J. Appl. Phys.* **2002**, *91*, 2896-2900.

4. Sui, G.G.; Wu, X.L.; Gu, Y.; Boa, X.M. *Appl. Phys. Lett.* **1999**, *74*, 1812-1814.

5. Tamura, H.; Ruckschloss, M.; Wirschem, T.; Veprek, S. *Appl. Phys. Lett.* **1994**, *65*, 1537-1539.

6. Kenyon, A.J.; Trwoga, P.F.; Pitt, C.W.; Rehm, G. J. Appl. Phys. **1996**, *79*, 9291-9300.

7. Lin, G.-R.; Lin, C.-J.; Lin, C.-K.; Chou, L.-J.; Chueh, Y.-L. *J. Appl. Phys.* **2005**, *97*, 094306.

8. Chen, X.Y.; Lu, Y.F.; Wu, Y.H.; Cho, B.J.; Liu, M.H.; Dai, D.Y.; Song, W.D. *J. Appl. Phys.* **2003**, *93*, 6311-6319.

9. Koch, F.; Petrova-Koch, V. *J. Non-Cryst. Solids* **1996**, *198-200*, 840-846.

10. Flores Gracia, F.; Aceves, M.; Carrillo, J.; Domínguez, C.; Falcony, C. *Superfices y Vacio* **2005**, *18*, 7-13.

11. Kohno, K.; Osaka, Y.; Toyomura, F.; Katayama, H. *Jpn. J. Appl. Phys.* **1994**, *33*, 6616-6622.

12. Kanzawa, Y.; Kageyama, T.; Takeoka, S.; Fujii, M.; Hayashi, S.; Yamamoto, K. *Solid State Commun.* **1997**, *102*, 533-537.

13. Kahler, U.; Hofmeister, H. *Appl. Phys. Lett.* **1999**, *75*, 641-643.

14. Rinnert, H.; Vergnat, M.; Marchal, G.; Burneau, A. *J. Lumin.* **1999**, *80*, 445-448.

15. Patrone, L.; Nelson, D.; Safarov, V.I.; Sentis, M.; Marine, W.; Glorico, S. *J. Appl. Phys.* **2000**, *87*, 3829-3837.

16. Sachenko, A.V.; Kaganovich, E.B.; Manoilov, E.G.; Svechnikov, S.V. *Semiconductors* **2001**, *35*, 1383-1389.

17. Rani, J.R.; Mahadevan, Pillai, V.P.; Ajimshav, R.S.; Jayaraj, M.K.; Jayasree, R.S. *J. Appl. Phys.* **2006**, *100*, 014302.

18. Komenkova, L.; Korsunska, N.; Sheinkman, M.; Stara, T.; Torchynska, T.V.; Vivas Hernandez, A. *J. Lumin.* **2005**, *115*, 117-121.

19. Wang, X.X.; Zhang, J.G.; Ding, L.; Cheng, B.W.; Ge, W.K.; Yu, J.Z.; Wang, Q.M. *Phys. Rev. B* **2005**, *72*, 195313.

20. Nesheva, D.; Raptis, C.; Perakis, A.; Bineva, I.; Aneva, Z.; Levi, Z.; Alexandrova, S.; Hofmeister, H. *J. Appl. Phys.* **2002**, *92*, 4678-4683.

21. Khomenkova, L.; Korsunska, N.; Yukhimchuk, V.; Jumayev, B.; Torchynska, T.; Vivas Hernandez, A.; Many, A.; Goldstein, Y.; Savir, E.; Jedrzejewski, J. *J. Lumin.* **2003**, *102-103*, 705-711.

22. Khriachtchev, L.; Novikov, S.; Lahtinen, J. *J. Appl. Phys.* **2002**, *92*, 5856-5862.

23. Fazio, B.; Vulpio, M.; Geradi, C.; Liao, Y.; Lombardo, S.; Trusso, S.; Neri, F. *J. Elec. Soc.* **2002**, *149*, G376-G378.

24. Soni, R.K.; Fonesca, L.F.; Resto, O.; Buzaianu, M.; Weisz, S.Z. *J. Lumin.* **1999**, *83-84*, 187-191.

25. Comedi, D.; Zalloum, O.H.Y.; Irving, E.A.; Wojcik, J.; Flynn, M.J.; Mascher, P. *J. Appl. Phys.* **2006**, *99*, 023518.

26. Islam, N.; Pradhan, A.; Kumar, S. *J. Appl. Phys.* **2005**, *98*, 24309.

27. Richter, H.; Wang, Z.P.; Ley, L. *Solid State Commun.* **1981**, *39*, 625-629.

28. Pankove, J.I., in: *Optical Process in Semiconductors*; Prentice Hall; Englewood; Cliffs; NJ; **1971** p. 34.

29. Khriachtchev, L.; Räsänen, M.; Novikov, S.; Kilpelä, O.; Sinkkonen, J. *J. Appl. Phys.* **1999**, *86*, 5601-5608.

30. Tsang, J.C.; Tischler, M.A.; Collins, R.T. *Appl. Phys. Lett.* **1992**, *60*, 2279-2281.

31. Chu, T.S.; Zhang, R.Q.; Cheung, H.F. *J. Phys. Chem. B* **2001**, *105*, 1705-1709.